

Integrated Sensing and Communication for Segmented Waveguide-Enabled Pinching Antenna Systems

Qian Gao, *Graduate Student Member, IEEE*, Ruikang Zhong, *Member, IEEE*,
Hyundong Shin, *Fellow, IEEE*, Yuanwei Liu, *Fellow, IEEE*

Abstract—In this paper, an integrated sensing and communication (ISAC) design for segmented waveguide-enabled pinching-antenna array (SWAN) systems is proposed to improve the performance of systems by leveraging the low in-waveguide propagation loss of segmented waveguides. The hybrid segment selection and multiplexing (HSSM) protocol is implemented to provide favorable performance with less hardware cost. To achieve this, a joint transmit beamforming optimization, segment selection, and pinching antenna positioning problem is formulated to maximize the sum communication rate with the constraints of sensing performance. To solve the maximization problem, we propose a segment hysteresis based reinforcement learning (SHRL) algorithm to learn segment selection and pinching antenna positions in different progress to explore better strategies. Simulation results demonstrate that 1) the proposed SWAN-ISAC scheme outperforms the other baseline schemes, and 2) the proposed HARL algorithm achieves better performance compared to conventional RL algorithms.

Index Terms—Integrated sensing and communication (ISAC), reinforcement learning (RL), pinching antenna, segmented waveguide.

I. INTRODUCTION

The rapid development of sixth-generation (6G) wireless networks is expected to enable a wide range of intelligent services such as autonomous driving, extended reality, and digital twin systems. To support these applications, networks must not only provide ultra-reliable high-rate communication but also acquire fine-grained awareness of the surrounding environment. Integrated Sensing and Communication (ISAC) [1] has therefore emerged as a key paradigm that allows communication and radar sensing to share the same hardware platform, spectrum, and signaling resources. By transmitting dual-functional waveforms, base stations can simultaneously deliver data to mobile users and probe the environment for target detection, localization, and tracking. This integration not only improves spectrum efficiency but also promotes tighter

Qian Gao is with the School of Electronic Engineering and Computer Science, Queen Mary University of London, London, E1 4NS, U.K. (e-mail: q.gao@qmul.ac.uk).

Ruikang Zhong is with the School of Information and Communication Engineering, Xi'an Jiaotong University, Xi'an 701149, P.R. China. (e-mail: ruikang.zhong@xjtu.edu.cn)

Hyundong Shin is with the Department of Electronics and Information Convergence Engineering, Kyung Hee University, 1732 Deogyoeng-daero, Giheung-gu, Yongin-si, Gyeonggi-do 17104, Republic of Korea. (e-mail: hshin@khu.ac.kr)

Yuanwei Liu is with the Department of Electrical and Electronic Engineering, The University of Hong Kong, Hong Kong. (e-mail: yuanwei@hku.hk).

cooperation between communication and sensing functions, which is crucial for vehicular networks, unmanned aerial systems, and industrial Internet-of-Things (IoT) scenarios [2].

A fundamental challenge for ISAC lies in the antenna hardware. Traditional phased-array or reconfigurable antennas [3], [4] can steer beams electronically, but they often suffer from high cost, complex feeding networks, and limited flexibility when adapting to dynamically changing user and target distributions. Recently, the concept of pinching antenna [5] has been introduced as a promising candidate for ISAC systems. A pinching antenna can be realized by directly “pinching” the waveguide or transmission line to form a radiation point. This design provides high spatial flexibility, as radiation points can be created at arbitrary positions along the waveguide. Compared with other types of flexible antennas, such as movable antennas [4] or fluid antennas [3], the pinching antenna exhibits lower hardware complexity, more efficient energy transfer, and the capability of forming multiple radiation points without complicated mechanical movement. These features make pinching antennas become an attractive enabler for ISAC, as they can improve the flexibility of joint optimization of beamforming and sensing coverage while reducing system cost.

However, existing pinching-antenna designs [6]–[8] are implemented on single or multiple tens-of-meters-long waveguides, which degrade system performance when covering a large region and lead to costly maintainability. To further enhance the flexibility of pinching antennas, recent studies have proposed the use of segmented waveguide-enabled pinching-antenna array (SWAN) systems [9]. In this architecture, the waveguide is physically divided into multiple segments, each of which can be selectively activated to serve as a controllable radiation aperture. The segmented design introduces a new degree of freedom, allowing more refined spatial resource allocation and reducing in-waveguide propagation loss.

Motivated by these benefits, this paper proposes the ISAC design for SWAN. Specifically, the hybrid segment selection and multiplexing (HSSM) protocol is implemented, where each segment is connected to one dedicated radio frequency (RF) chain and segments are selected to realize multiplexing with less hardware cost. Then, the ISAC performance can be maximized by optimizing the transmit beamforming, segment selection, and pinching antenna positions. A segment hysteresis based reinforcement learning (SHRL) algorithm is proposed to tackle the non-convex optimization problem.

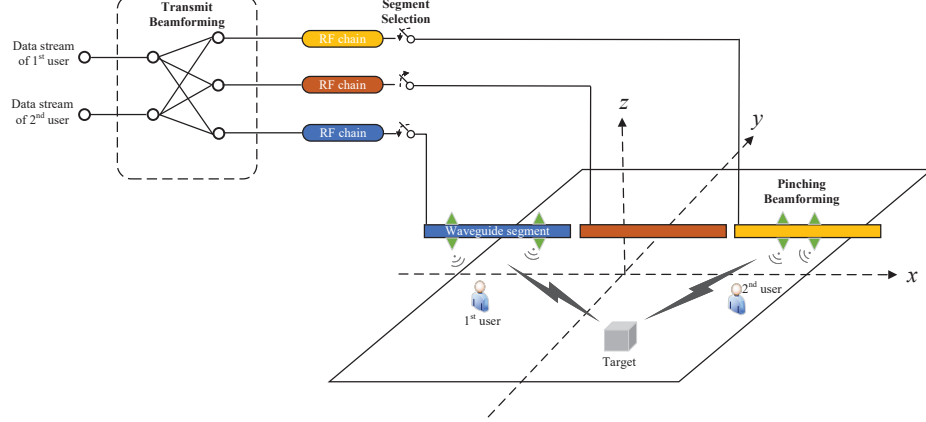


Fig. 1: Illustration of SWAN-ISAC, $M = 3, N = 4, K_c = 2, K_s = 1$.

II. SYSTEM MODEL AND PROBLEM FORMULATION

In this paper, we investigate the downlink SWAN-ISAC system, as shown in Fig. 1. We assume that base station (BS) is equipped with M segmented waveguides, each with length L , to jointly serve K_c single-antenna communication users and detect K_s sensing targets. Each waveguide contains N pinching antennas (PAs), resulting in $M \times N$ total antennas. The positions of the n th PA on the m th waveguide can be denoted as $\psi_n^m = (x_n^m, y_n^m, d)$, where d is the fixed waveguide height above the x - y plane. The feed point of each waveguide is assumed to be the front-left end of each waveguide. Communication users and sensing targets are located in the x - y plane, with coordinates $\psi_{k_c} = (x_{k_c}, y_{k_c}, 0)$ and $\psi_{k_s} = (x_{k_s}, y_{k_s}, 0)$, respectively.

A. Signal Model

Compared to the time-division multiple access (TDMA) scheme used in single waveguide and multiple systems, the segmented waveguides can be connected to dedicated RL chains to enable maximal ratio transmission (MRT) in the downlink. The transmitted signal for the m th waveguide is denoted as

$$s_m = \sum_{k_c=1}^{K_c} \mathbf{W}_{k_c, m} \cdot z_{k_c}, \quad (1)$$

where z_{k_c} is the transmitted signal symbol for the k_c th user, $\mathbf{W} \in \mathbb{C}^{K_c \times M}$ is the transmit beamforming.

Then, this signal is fed into the corresponding waveguide for pinching beamforming. For each waveguide, the signals transmitted by PAs are phase-shifted versions of each other. Considering the in-waveguide loss, the radiation signal can be expressed as

$$\mathbf{s}_m = s_m \begin{bmatrix} \sqrt{\frac{P_m}{N}} 10^{-\frac{\kappa}{20} \|\psi_0^m - \psi_1^m\|} e^{-j\theta_1^m} \\ \vdots \\ \sqrt{\frac{P_m}{N}} 10^{-\frac{\kappa}{20} \|\psi_0^m - \psi_N^m\|} e^{-j\theta_N^m} \end{bmatrix}^T \quad (2)$$

where P_m is the feed power on m th waveguide, θ_n^m is the signal phase shift at n -th PA and $\theta_n^m = 2\pi \frac{|\psi_0^m - \psi_n^m|}{\lambda_0}$. Thereof,

ψ_0^m is the feed point of m th waveguide, $\lambda_0 = \frac{\lambda}{n_{\text{eff}}}$ is the waveguide wavelength in a dielectric waveguide, n_{eff} is the effective refractive index and λ represents wavelength. It is assumed that transmit power is allocated to N pinching antennas evenly and this results in the scaling factor of $\sqrt{\frac{1}{N}}$.

Since the employment of PAs provides LoS channel conditions for ISAC, the near-field spherical wave channels for communication user k_c and sensing target k_s can be expressed as

$$\mathbf{h}_{k_c, m} = \left[\frac{\alpha e^{-j \frac{2\pi}{\lambda} \|\psi_{k_c} - \psi_1^m\|}}{\|\psi_{k_c} - \psi_1^m\|}, \dots, \frac{\alpha e^{-j \frac{2\pi}{\lambda} \|\psi_{k_c} - \psi_{N, t}^m\|}}{\|\psi_{k_c} - \psi_{N, t}^m\|} \right]^T, \quad (3)$$

and

$$\mathbf{h}_{k_s, m} = \left[\frac{\alpha e^{-j \frac{2\pi}{\lambda} \|\psi_{k_s} - \psi_1^m\|}}{\|\psi_{k_s} - \psi_1^m\|}, \dots, \frac{\alpha e^{-j \frac{2\pi}{\lambda} \|\psi_{k_s} - \psi_{N, t}^m\|}}{\|\psi_{k_s} - \psi_{N, t}^m\|} \right]^T, \quad (4)$$

where $\alpha = \frac{c}{4\pi f_c}$ is a constant that depends on the speed of light c and the carrier frequency f_c , $\psi_{k, t}$ and $\psi_{l, t}$ denote the location of user k and target l in time slot t , respectively.

B. Communication and Sensing Metrics

The received signal at communication user k_c is $y_{k_c} = \sum_{m=1}^M \mathbf{h}_{k_c, m}^T \mathbf{s}_m + \sum_{m=1}^M \sum_{k'_c=1, k'_c \neq k_c}^{K_c} \mathbf{h}_{k_c, m}^T \mathbf{s}'_m + n$, where n represents the additive Gaussian noise.

Then, the data rate of user k can be expressed as

$$R_{k_c} = B \log_2 \left(1 + \frac{\sum_{m=1}^M |\mathbf{h}_{k_c, m}^T \mathbf{s}_m|^2}{\sum_{m=1}^M \sum_{k'_c=1, k'_c \neq k_c}^{K_c} |\mathbf{h}_{k_c, m}^T \mathbf{s}'_m|^2 + \sigma^2} \right), \quad (5)$$

where σ^2 is the noise power and B represents bandwidth.

The communication signals are further exploited for targets' sensing. The illumination power is used as the sensing performance metric, which can be expressed as

$$\Gamma_{k_s} = \mathbb{E} \left[\sum_{m=1}^M |\mathbf{h}_{k_s, m}^T \mathbf{s}_m|^2 \right]. \quad (6)$$

To fulfill the requirements of sensing quality, the illumination towards different sensing targets needs to consider the minimum threshold $\tilde{\Gamma}$.

C. Problem Formulation

Based on the above system model, we formulate the joint optimization of the pinching beamforming $\{\psi_n^m\}$, the segment selection $\{\phi_m\}$, and the transmit beamforming $\{\mathbf{W}_{k_c, m}\}$ to maximize the total communication data rate across all users while satisfying sensing threshold. The optimization problem is:

$$\begin{aligned} \max_{\{\psi_n^m, \phi_m, \mathbf{W}_{k_c, m}\}} \quad & \sum_{k_c=1}^{K_c} R_{k_c} \\ \text{s.t.} \quad & \Gamma_{k_s} \geq \tilde{\Gamma}, \quad \forall k_s \in \{1, \dots, K_s\}, \end{aligned} \quad (7a)$$

$$|\mathbf{W}|^2 = \sum_{m=1}^M \mathbf{P}_m \leq \mathbf{P}, \quad \forall m, \quad (7b)$$

$$\phi_m \in [0, 1], \quad \forall m, \quad (7c)$$

$$\|\psi_n^m - \psi_{n'}^m\| \geq \delta, \quad \forall n \neq n', \forall m, n. \quad (7d)$$

Constraint (7a) ensures the minimum SNR requirement for target sensing, constraints (7b) and (7c) enforce the total transmit power and the range of segment selection, respectively. Constraint (7d) guarantees the minimum spacing between any two pinching antennas. This optimization problem is nonlinear and non-convex due to the presence of fractional illumination power expressions, absolute values, and exponential phase terms.

III. PROPOSED SEGMENT HYSTERESIS BASED REINFORCEMENT LEARNING SOLUTION

In this section, we introduce the Segment-Hysteresis Reinforcement Learning (SHRL) framework, which is specifically designed for ISAC systems employing segmented waveguides. Different from conventional RL approaches that update segment selections independently at each step, SHRL introduces a hysteresis-based segment-update mechanism that stabilizes the agent's decisions by preventing abrupt changes in the antenna-segment mapping. This mitigates the non-stationarity caused by rapid structural switching and significantly improves learning stability.

The core idea of SHRL is to integrate a probabilistic hysteresis gate into the segment-selection process so that new segment decisions are only accepted when they provide sufficiently large improvement or when a certain hysteresis threshold is exceeded. Otherwise, previous selections are retained. This mechanism enforces temporal consistency and enables smooth policy exploration in the SWAN-ISAC optimization task.

A. MDP Formulation with Segment Hysteresis

The SHRL framework operates within a single unified environment \mathcal{E} that comprises all antenna elements and segmented waveguide modules. The MDP is defined as follows.

State Space \mathcal{S} : At each time step t , the system state is represented by

$$\mathbf{s}_t = [\mathbf{h}_{k_c, t}, \mathbf{h}_{k_s, t}, \psi_{t-1}, \phi_{t-1}],$$

including the communication and sensing CSI, the previous antenna positions ψ_{t-1} , and the previous segment assignments ϕ_{t-1} , which are essential for the hysteresis mechanism.

Action Space \mathcal{A} : The agent outputs continuous-valued updates for

$$\mathbf{a}_t = [\psi_t, \phi_t, \mathbf{W}_t],$$

where ϕ_t represents the raw segment-selection logits. Before executing ϕ_t , a hysteresis filter is applied to determine whether segment reassignment should occur.

Reward Function \mathcal{R} : The reward encourages high communication throughput while satisfying sensing-SNR constraints:

$$r_t = \sum_{k_c=1}^{K_c} R_{k_c, t} - \sum_{k_s=1}^{K_s} \mathbb{I}_{\{\Gamma_{k_s, t} < \tilde{\Gamma}\}}.$$

B. Segment Hysteresis Mechanism

Given the raw segment logits ϕ_t from the actor, SHRL determines the final segment assignment $\tilde{\phi}_t$ according to:

$$\tilde{\phi}_{m, t} = \begin{cases} \phi_{m, t}, & \text{with probability } p_{\text{update}}, \\ \tilde{\phi}_{m, t-1}, & \text{otherwise,} \end{cases}$$

where $p_{\text{update}} \in (0, 1)$ is the hysteresis probability controlling the update frequency. A small p_{update} preserves stability, while a larger value allows more aggressive exploration. This mechanism prevents frequent remapping of antennas across segments, thereby reducing structural variance and improving the convergence behavior of the policy.

C. Training Procedure

We employ the Advantage Actor-Critic (A2C) algorithm [10] to optimize the SHRL policy. The actor outputs both beamforming parameters and raw segment logits, while the hysteresis gate refines the segment-selection action before it is applied to the environment. The critic evaluates state values and guides policy updates.

After training convergence, the learned policy π_{θ^*} is used for real-time control of antenna positions, beamforming weights, and hysteresis-smoothed segment selection.

The SHRL approach provides an effective balance between exploration efficiency and structural stability, making it particularly suitable for large-scale modular ISAC architectures. By smoothing segment transitions through hysteresis, SHRL achieves more stable convergence compared with conventional RL baselines, while maintaining high communication-sensing performance.

IV. SIMULATION RESULTS

In this section, we conduct experimental simulations for the proposed SWAN-ISAC deployment and SHRL algorithm. In the simulation, we consider a multi-user ISAC system with a configurable pinching antenna deployment geometry, where

Algorithm 1 SHRL: Reinforcement Learning with Segment Hysteresis

```

1: Initialize policy  $\pi_\theta$ , critic  $V_\psi$  and hysteresis memory  $\tilde{\phi}_0$ .
2: for each episode do
3:   Reset environment and observe initial state  $s_0$ .
4:   for each step  $t$  do
5:     Sample raw action  $a_t = \pi_\theta(s_t)$ , extract raw segment logits  $\phi_t$ .
6:     Apply hysteresis gate:
7:      $\tilde{\phi}_t = \begin{cases} \phi_t, & \text{with prob. } p_{\text{update}}, \\ \tilde{\phi}_{t-1}, & \text{otherwise.} \end{cases}$ 
8:     Execute action  $(\psi_t, \tilde{\phi}_t, \mathbf{W}_t)$  in the environment.
9:     Observe  $r_t$  and  $s_{t+1}$ .
10:    Update critic and actor using A2C:
11:     $\mathcal{L}_V = (V_\psi(s_t) - \hat{R}_t)^2$ ,  $\mathcal{L}_\pi = \log \pi_\theta(a_t|s_t) \hat{A}_t$ .
12:    Store updated  $\tilde{\phi}_t$ .
13:   end for
14: end for
15: Output the final policy parameters  $\theta^*$ .

```

$U = 6$ users and $T = 1$ target are randomly distributed within a $50\text{ m} \times 60\text{ m}$ area at ground level. The antenna array of each segment consists of $N = 10$ elements. The carrier frequency is set to $f = 28\text{ GHz}$, and each antenna element is allowed to adjust its position under a minimum inter-element spacing $\delta = \lambda/2$. Communication channels are modeled as LoS paths with effective refractive index $n_{\text{eff}} = 1.4$. The total power constraint is $P_{\text{max}} = 100\text{ W}$ and the height of waveguides is 5m. The communication data rate is computed based on coherent beamforming with additive white Gaussian noise power of -90 dBm , and the sensing performance is evaluated via the maximum illumination power achieved for the target. The sensing threshold $\tilde{\Gamma}$ is set to -20 dBm .

To evaluate the performance of the proposed SHRL algorithm, we adapt four benchmarks as follows:

- **SPRL:** Segment periodical selection is a variant of the proposed SHRL algorithm, where segment selection are made in a fixed period. In this paper, we got period 5 with grid search.
- **A2C:** This is a synchronous policy-gradient algorithm where a single actor selects actions and a critic estimates the value function. It updates the policy using the advantage signal.
- **PPO:** PPO improves policy-gradient updates by constraining the step size using a clipped surrogate objective. This prevents overly large policy updates and provides better stability and robustness than vanilla actor-critic or A2C, especially in high-dimensional or multi-agent settings..
- **Random scheme:** This scheme requires the agent to execute random actions within predefined regions.

Fig. 2 compares the ISAC performance of the SWAN (HSSM and SM protocols) against the conventional PASS scheme under two representative cases. In the sparse case, where users and targets are spatially separated, both SWAN-HSSM and SWAN-SM achieve significantly higher rewards than PASS. SWAN-HSSM exhibits the highest final reward,

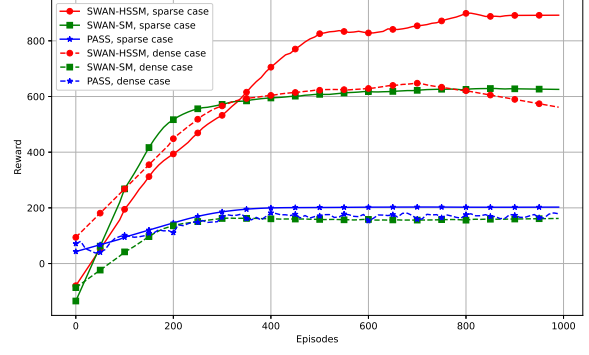


Fig. 2: ISAC performance comparison between SWAN and PASS under two different cases.

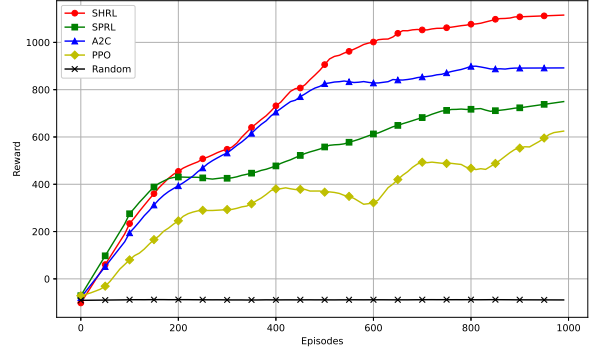


Fig. 3: Performance comparison of SWAN-ISAC under different algorithms.

owing to its ability to selectively activate effective segments and reduce unnecessary power spreading. SWAN-SM also performs well but remains slightly inferior due to the lack of hybrid-selective control. In contrast, PASS yields limited performance because its power allocation mechanism does not exploit spatial diversity.

In the dense case, where users and targets are located close to each other, the reward of all schemes decreases. This degradation is attributed to stronger multi-user interference and reduced beamforming separability. However, SWAN-HSSM still maintains a notable advantage over SWAN-SM and PASS, as selective segment activation helps mitigate propagation loss and suppress interference. PASS continues to show the lowest performance across both cases due to its fixed, non-adaptive structure.

Fig. 3 compares the learning performance of different reinforcement learning strategies for SWAN-ISAC. SHRL, which introduces probabilistic hysteresis for segment updating, achieves the highest reward and the most stable convergence by preventing unnecessary segment switching. A2C ranks second, benefiting from more consistent policy updates in this continuous control setting. SPRL, which updates segments only at fixed intervals, converges more slowly and reaches a lower performance ceiling due to reduced exploration flexibil-

TABLE I: ISAC performance comparison of different algorithms under varying waveguide configurations.

(a) Fixed segment number $M = 3$, varying total waveguide length L_{wg} .

L_{wg}	SHRL	SPRL	A2C	PPO	Random
40 m	13.15/1.09e - 5	7.71/1.05e - 5	9.93/1.12e - 5	6.37/1.18e - 5	3.05/9.19e - 6
60 m	13.56/1.26e - 5	11.20/1.28e - 5	11.63/1.24e - 5	9.45/1.30e - 5	3.09/3.11e - 6
80 m	17.07/1.34e - 5	11.32/1.42e - 5	13.85/1.37e - 5	10.86/1.45e - 5	3.55/2.77e - 6
100 m	6.41/1.10e - 5	3.36/1.23e - 5	4.58/1.17e - 5	4.55/1.26e - 5	2.95/1.81e - 6

(b) Fixed total waveguide length $L_{wg} = 40m$, varying segment number M .

M	SHRL	SPRL	A2C	PPO	Random
3	13.15/1.09e - 5	7.71/1.05e - 5	9.93/1.12e - 5	6.37/1.18e - 5	3.05/9.19e - 6
6	12.91/2.74e - 5	6.64/2.28e - 5	8.97/1.76e - 5	5.98/1.54e - 5	3.03/5.92e - 6
9	11.82/3.72e - 5	6.36/2.42e - 5	8.32/2.02e - 5	5.64/1.68e - 5	2.83/4.44e - 6
12	10.59/4.96e - 5	5.42/3.54e - 5	7.63/2.64e - 5	5.15/1.78e - 5	3.00/3.96e - 6

ity. PPO performs worse because its clipping mechanism over-constrains policy updates in this multi-parameter environment. As expected, the Random policy fails to learn any meaningful behavior. Overall, SHRL provides the most effective balance between exploration stability and segment-control flexibility, leading to the best ISAC performance.

Table I summarizes the ISAC performance of different algorithms under varying waveguide configurations. Each entry in the table is presented in the form “ R/Γ ”, where the first value denotes the total communication rate (in bps/Hz), and the second value denotes the achieved sensing performance (in dB). In Table I(a), the segment number is fixed to $M = 3$ while the total waveguide length L_{wg} varies. Across all configurations, SHRL consistently achieves the highest communication rate and maintains sensing SNR closest to the required threshold. As L_{wg} increases from 40 m to 80 m, all methods exhibit performance improvements due to the larger available spatial aperture. However, for very long waveguides (e.g., $L_{wg} = 100$ m), the propagation loss becomes innegligible, resulting in performance degradation across all algorithms. SHRL remains the most robust in this high-loss regime, whereas SPRL and PPO suffer more substantial degradation. Random selection performs poorly in all cases, confirming the necessity of intelligent segment control and beamforming. Table I(b) fixes the total waveguide length at $L_{wg} = 40$ m and varies the segment number M . The sensing SNR improves with larger M because shorter per-segment waveguides experience lower in-waveguide attenuation, leading to stronger coherent reflection at the target. Conversely, the communication rate decreases since more segments reduce the number of antennas per segment, degrading the effective array gain and weakening the communication beamforming. Among all methods, SHRL consistently achieves the best balance between sensing and communication performance. For the random scheme, its sensing illumination power cannot meet the minimum threshold, which guarantees the sensing metric to be considered during the training of other algorithms.

V. CONCLUSION

In this paper, we proposed a SWAN-enhanced ISAC framework that exploits the spatial diversity of segmented waveguides to enable flexible beamforming and efficient separation between communication and sensing. By formulating the joint optimization of antenna positioning, segment assignment, and

transmit beamforming as a Markov decision process, we developed a SHRL algorithm capable of stabilizing segment transitions while maintaining exploration efficiency. Compared with existing baselines such as SPRL, A2C, and PPO, the proposed SHRL method achieves superior learning stability and higher ISAC performance, owing to its effective handling of segment update dynamics and task-specific structural priors. Simulation results demonstrate that the SWAN-ISAC architecture maintains the sensing SNR near its operational threshold while significantly boosting communication throughput. These findings highlight the advantages of segmented-waveguide antenna systems and validate their potential for high-performance, power-limited ISAC deployments.

REFERENCES

- [1] F. Liu, Y. Cui, C. Masouros, J. Xu, T. X. Han, Y. C. Eldar, and S. Buzzi, “Integrated sensing and communications: Toward dual-functional wireless networks for 6G and beyond,” *IEEE J. Sel. Areas Commun.*, vol. 40, no. 6, pp. 1728–1767, 2022.
- [2] Q. Gao, R. Zhong, H. Shin, and Y. Liu, “MARL-based UAV trajectory and beamforming optimization for ISAC system,” *IEEE Internet Things J.*, vol. 11, no. 24, pp. 40 492–40 505, 2024.
- [3] K.-K. Wong, A. Shojaeifard, K.-F. Tong, and Y. Zhang, “Fluid antenna systems,” *IEEE Trans. Wirel. Commun.*, vol. 20, no. 3, pp. 1950–1962, 2021.
- [4] L. Zhu, W. Ma, and R. Zhang, “Modeling and performance analysis for movable antenna enabled wireless communications,” *IEEE Trans. Wirel. Commun.*, vol. 23, no. 6, pp. 6234–6250, 2024.
- [5] Z. Ding, R. Schober, and H. Vincent Poor, “Flexible-antenna systems: A pinching-antenna perspective,” *IEEE Trans. Commun.*, pp. 1–1, 2025.
- [6] Y. Xu, Z. Ding, and G. K. Karagiannidis, “Rate maximization for downlink pinching-antenna systems,” *IEEE Wirel. Commun. Lett.*, vol. 14, no. 5, pp. 1431–1435, 2025.
- [7] S. A. Tegos, P. D. Diamantoulakis, Z. Ding, and G. K. Karagiannidis, “Minimum data rate maximization for uplink pinching-antenna systems,” *IEEE Wirel. Commun. Lett.*, vol. 14, no. 5, pp. 1516–1520, 2025.
- [8] X. Xu, X. Mu, Y. Liu, and A. Nallanathan, “Joint transmit and pinching beamforming for pinching antenna systems (PASS): Optimization-based or learning-based?” *arxiv:2502.08637*, 2025.
- [9] C. Ouyang, H. Jiang, Z. Wang, Y. Liu, and Z. Ding, “Uplink and downlink communications in segmented waveguide-enabled pinching-antenna systems (SWANs),” *arXiv:2509.10666*, 2025.
- [10] M. Volodymyr, A. P. Badia, M. Mehdi, G. Alex, L. Timothy P, H. Tim, S. David, and K. Koray, “Asynchronous methods for deep reinforcement learning,” *arXiv:1602.01783*, 2016.